European Journal of Wood and Wood Products (2019) 77:1021–1028
https://doi.org/10.1007/s00107-019-01463-2

ORIGINAL

Significant and reversible dimensional changes in hydrothermally compressed cedar wood and its potential as humidity-sensitive actuator

Eiichi Obataya[1] · **Shuoye Chen**[2]

Received: 24 January 2019 / Published online: 20 September 2019
© Springer-Verlag GmbH Germany, part of Springer Nature 2019

Abstract
Japanese cedar wood samples were radially compressed by 52% using saturated water vapor at 160 °C. The steam-compressed (SC) samples were boiled in water to recover their compressed shapes, and the shape recovery was evaluated on the basis of the dimensional changes under completely dry condition. The compressed shape of the wood was memorized by steaming for 90 min. After the recovery treatment, the radial and tangential swelling of the wood samples were measured during the moistening and subsequent drying. The SC wood exhibited anomalously large and reversible swelling in the radial direction, whereas its tangential swelling was almost the same as that of the uncompressed wood. The significant and reversible swelling of the SC wood was due to the swimming ring-like expansion and collapse of the folded earlywood cell wall. To evaluate the potential of SC wood as a humidity-sensitive actuator, a wooden bilayer was made by combining SC wood with a cedar wooden veneer. The flexural deformation of the SC wooden bilayer due to humidity change was significantly greater than that of the conventional bilayer, which consists of beech wood and cedar wooden veneer.

1 Introduction

Transverse compression enables the densification of soft coniferous lumber to a stiffer material (Seborg and Stamm 1941; Inoue et al. 1990, 1993; Ito et al. 1998a, b; Dwianto et al. 1998; Navi and Girardet 2000; Kutnar et al. 2009; Fang et al. 2012; Sandberg et al. 2013). When a wood is simply compressed, its compressed shape is mostly recovered by re-wetting, boiling in water and drying. However, such a shape recovery can be effectively prevented by compression under high-temperature steam (Inoue et al. 1993). By using this method, which is referred to as steam-compression, the compressed shape of wood in dry condition can be effectively memorized, and it remains unchanged after re-wetting, boiling in water and drying. The steam-compression is widely used for the densification and the three-dimensional molding of wood, as it provides a faster shape fixation with minimal color change (Ito et al. 1998a, b; Navi and Girardet 2000).

There have been several discussions on the mechanism of the shape fixation by steaming. Hydrophobization is generally considered as a major mechanism of shape fixation by steaming. Steaming causes the depolymerization of polysaccharides, the decomposition and subsequent condensation of lignin, and the crystallization of cellulose (Wikberg and Maunu 2004; Inagaki et al. 2010; Yin et al. 2011, 2017; Kuribayashi et al. 2016; Guo et al. 2015, 2016, 2017). All these changes reduce the hygroscopicity of wood to a certain extent, and the reduced hygroscopicity indirectly prevents the shape recovery due to the hygrothermal softening of amorphous wood polymers. However, perfect fixation is not achieved when wood is steamed and then compressed (Inoue et al. 2008). In addition, the hygroscopicity of wood at high relative humidity (RH) levels is not significantly reduced by steaming (Obataya et al. 2002; Guo et al. 2015). The discussion above suggests that the reduced hygroscopicity cannot completely explain the shape fixation by steaming. A slip-cure concept was recently proposed, in which the structural changes in the crystalline cellulose were considered as a major mechanism underlying the shape fixation (Chen et al. 2018). It offers an explanation for the shape fixation

✉ Eiichi Obataya
obataya.eiichi.fu@u.tsukuba.ac.jp

[1] Graduate School of Life and Environmental Sciences, Tsukuba University, Tsukuba, Ibaraki 305-8572, Japan

[2] Graduate School of Bioagricultural Sciences, Nagoya University, Furo-cho, Chikusa-ku, Nagoya 464-8601, Japan

and changes in the mechanical properties of wood by the combination of compression and steaming.

A currently major issue is the dimensional instability of steam-compressed (SC) wood. By the steam compression, the dry dimension of wood can be memorized and it remains unchanged after boiling in water and drying. However, the SC wood exhibits anomalously large dimensional change during moistening and drying, given by the swimming ring-like deformation of the folded earlywood cells (Obataya and Chen 2018). Such a dimensional instability should be further investigated and considered in applications.

On the other hand, the dimensional instability of SC wood may be advantageous for its use as a humidity-sensitive wooden actuator. Rüggeberg and Burgert (2015) recently demonstrated the flexural deformation of a wooden bilayer beam under various humidity levels, and then proposed that the wooden bilayer allows for an automatic and low-cost actuation of the solar panel in response to the daily fluctuation of the environmental humidity. If the dimensional changes in SC wood are reversible and greater than those of the conventional actuation material such as beech wood, the SC wood expands the applicability of the wooden bilayer.

In this study, the significant swelling and shrinkage of SC cedar wood by wetting and drying was evaluated, and the reversibility of the swimming ring-like cellular deformation was confirmed. The humidity response of the SC wooden bilayer was then compared with that of the conventional bilayer, to demonstrate the potential of SC wood as a humidity-sensitive actuator.

2 Materials and method

2.1 Steam-compression

Figure 1a presents the shapes of the tested wood samples. Japanese cedar wood (*Cryptomeria japonica*) was cut into blocks with dimensions of 29 mm (longitudinal, L) × 29 mm (tangential, T) × 29 mm (radial, R). The average density of the samples under the completely dry condition was 362 kg/m^3. The samples were soaked in water at 25 °C for 1 week, and the water-swollen samples (31 mm in the R direction) were compressed in the R direction by 52% (to be 15 mm in the R direction) in an autoclave at 160 °C for 15 min, 30 min, 60 min, 90 min, 120 min, and 240 min. The inner volume of the autoclave was 1400 cm^3 (20 × 20 × 3.5 cm). The autoclave was filled with saturated water vapor and the internal pressure was maintained throughout steam-compression. After steam-compression, the leak valve was opened to release the pressurized water vapor and the

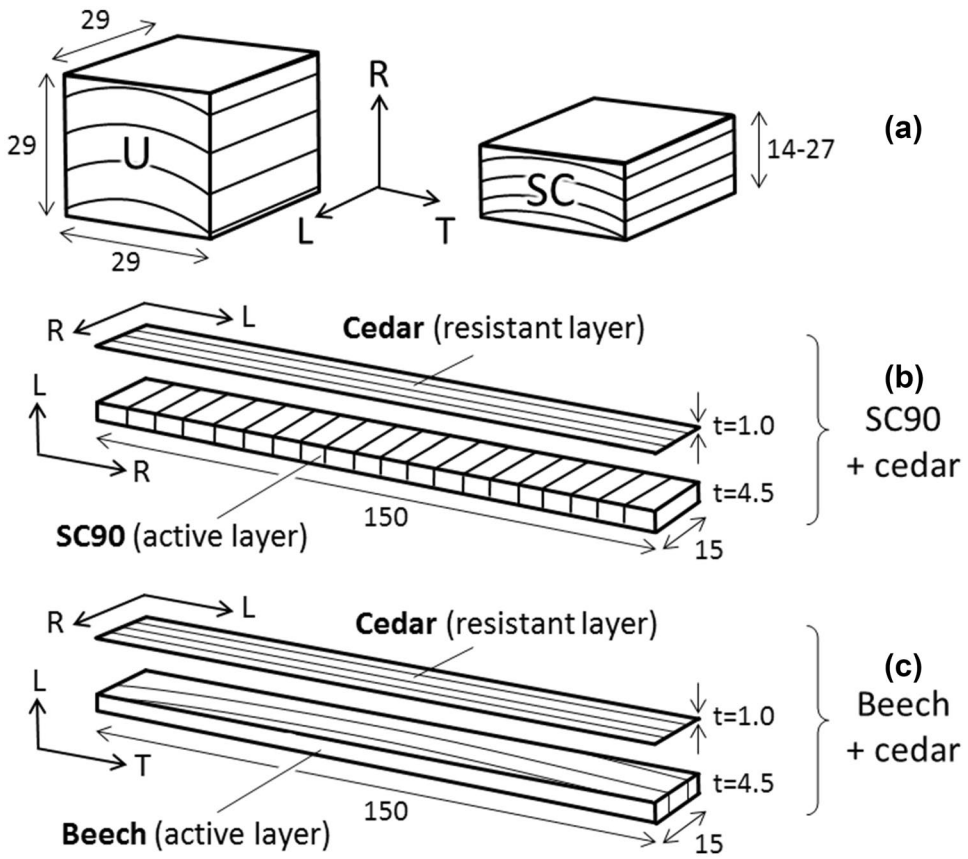

Fig. 1 Shape and fiber alignment of tested wood samples. **a** Uncompressed (U) and steam-compressed (SC) wood samples for shape recovery test; **b** bilayer beam consisting of SC wood steamed for 90 min (SC90) and cedar wooden veneer; and **c** conventional bilayer beam consisting of beech wood and cedar wooden veneer. Values indicate dimensions in mm

autoclave was immediately cooled to 100 °C. The samples, which remained compressed, were dried in the autoclave at 100 °C for 12–18 h. Thereafter, the wood samples were completely dried in an oven at 105 °C, and their dry masses and dimensions were measured. Twenty samples were used for each treatment condition.

2.2 Recovery test

The SC blocks were cut into thinner samples with dimensions of 10 mm (L) × 29 mm (T) × 14–27 mm (R). The samples were soaked in water at 25 °C for 1 week, and then boiled in water at 95 °C for 1 h for shape recovery. After the recovery treatment, the samples were air-dried at 25 °C and 60% relative humidity (RH) for more than 1 week, followed by oven-drying at 105 °C for 1 day, to determine their recovered dimensions (14–27 mm in the R direction) under the completely dry condition. Figure 2 illustrates the changes in the shapes of the wood samples by the steam compression and the subsequent recovery treatment. The recovery of the compressive strain (SR) was evaluated using the following equation:

$$\mathrm{SR} \equiv \frac{t_\mathrm{R} - t_\mathrm{C}}{t_0 - t_\mathrm{C}} \tag{1}$$

where t_0, t_C, and t_R are the completely dry thicknesses of the uncompressed, SC, and recovered samples in the R direction, respectively. The SR value is 1 for perfect shape recovery (no shape fixation) and 0 for no shape recovery (perfect shape fixation). Twenty samples were used for each treatment condition.

2.3 Observation of swelling and shrinkage of wood samples

After the recovery test, the wood samples were completely re-dried at 25 °C using P_2O_5. The densities of the completely dry SC samples (384–706 kg/m^3 depending on the steaming duration) were greater than that of the original wood (362 kg/m^3), because the compressed shape of the wood was memorized by the steaming. The equilibrium moisture content (EMC) and dimensions of the samples were measured stepwise during the moistening at 25 °C and 33% RH, 60% RH, 75% RH, 93% RH, and 97% RH, and then the samples were soaked in water for 1 week. Thereafter, the samples were dried stepwise at 25 °C and 97% RH, 93% RH, 75% RH, 60% RH, 33% RH, and 0% RH, while measuring their masses and dimensions. The conditioning time was 1 month at 60% RH or below, and 2 months at 75% RH or above. In this swelling-shrinkage test, four samples were used with SR values close to the average SR value of all (twenty) samples for each treatment condition. The swelling-shrinkage test was also conducted on nine hardwood species, namely, *Castanea crenata* (W1, 442 kg/m^3), *Quercus crispula* (W2, 470 kg/m^3), *Fagus crenata* (W3, 533 kg/m^3), *Cerasus jamasakura* (W4, 620 kg/m^3), *Acer pictum* (W5, 668 kg/m^3), *Juglans nigra* (W6, 684 kg/m^3), *Quercus acuta* (W7, 771 kg/m^3), *Guibourtia tessmannii* (W8, 814 kg/m^3), and *Eusideroxylon zwageri* (W9, 860 kg/m^3). The dimensions of the hardwood samples were 10 mm (L) × 30 mm (T) × 30 mm (R) under the air dry condition. Four samples were used for each wood species. For a portion of the uncompressed and SC wood samples, their cross sections were flattened using a microtome, and then observed using an optical microscope during three repeated wetting and drying cycles: wetting in water at 25 °C and oven drying at 105 °C. The radial (ΔR) and tangential (ΔT) swelling of wood sample are defined as

$$\Delta R\ (\%) \equiv 100 \times \frac{R - R_0}{R_0}, \tag{2}$$

$$\Delta T\ (\%) \equiv 100 \times \frac{T - T_0}{T_0}, \tag{3}$$

where R and T are the radial and tangential dimensions of wood in moistened condition, and R_0 and T_0 are those in absolutely dry condition, respectively.

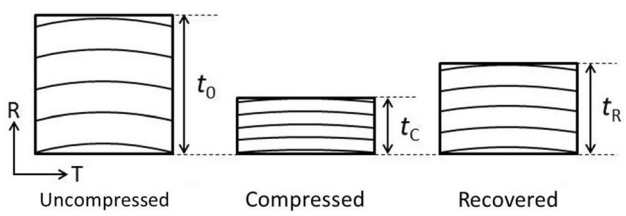

Fig. 2 Changes in the shape of cedar wood sample by steam compression and the subsequent recovery treatment

2.4 Observation of bilayer beams under humidity change

After the swelling-shrinkage test, the SC wooden blocks steamed for 90 min (SC90) were conditioned at 25 °C and 60% RH for longer than 1 month, and then their LT planes were glued using an epoxy resin (Araldite rapid, Huntsman Advanced Materials), as their R directions were aligned along the longitudinal direction. Thereafter, the glued beam was combined with a cedar wooden veneer with a thickness of 1 mm, and then cut into a bilayer beam with dimensions of 150 mm (length) × 15 mm (width) × 5.5 mm (height), as shown in Fig. 1b. Moreover, an unmodified beech wooden beam and cedar veneer were also combined into a bilayer beam. In this conventional bilayer beam, the T direction of

the beech wood was aligned along the longitudinal direction of the beam, as shown in Fig. 1c. The dimensions of the beech + cedar bilayer were the same as those of the SC90 + cedar bilayer.

The bilayer beams were then moistened at 25 °C and 97% RH for 12 h in a closed box, and then dried at 25 °C and 25% RH for 12 h, to observe the range of their flexural deformation under ambient conditions. Thereafter, the bilayer beams were exposed to uncontrolled outdoor conditions from the 4th–7th December 2017, in Tsukuba, Japan. The flexural deformations of the beams were observed at intervals of 30 min using a digital camera, and the temperature and RH near the beams were recorded using an environmental data logger (T&D Co, TR-72wf-S). The curvature radius (r) was measured on the captured images, and the curvature of beam was defined as $1/r$ in this study.

3 Results and discussion

3.1 Reversible swelling and shrinkage of SC wood

Figure 3 presents the SR values plotted against the steaming duration. As described in a previous report (Obataya and Chen 2018), the compressed shape of the cedar wood was almost completely fixed by steaming for 90 min or longer. However, the term "shape fixation" or "shape memory" does not mean dimensional stabilization: it means that the dry dimension of compressed wood remains unchanged after boiling in water. Even after the complete shape fixation (SR = 0), the SC wood shows significant dimensional change when it is moistened and dried. Figure 4 shows the radial swelling and shrinkage of the uncompressed wood and SC wood steamed for 90 min (SC90) as a function of the EMC.

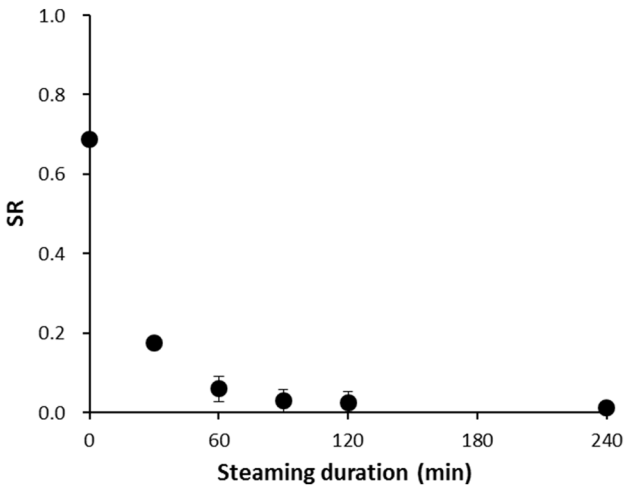

Fig. 3 Average strain recovery (SR) of SC cedar wood plotted against steaming duration. Bars indicate the standard deviations

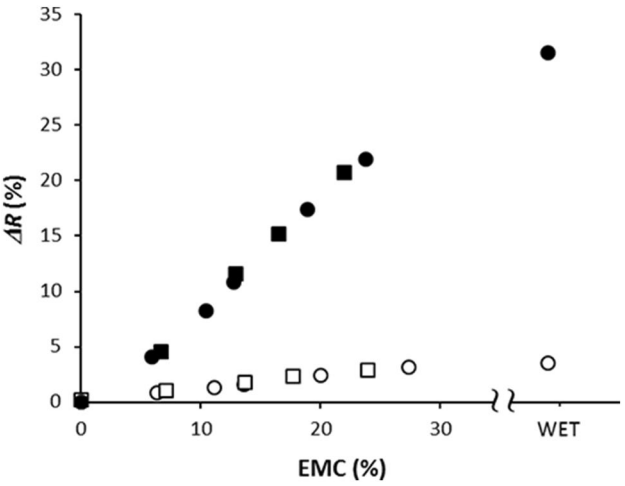

Fig. 4 Swelling in R direction (ΔR) of cedar wood samples as a function of equilibrium moisture content (EMC). Open plots, uncompressed; filled plots, steam-compressed for 90 min (SC90); circles, swelling (moistening) process; squares, shrinking (drying) process, standard deviation was less than 0.1% for the uncompressed wood or 0.4% for the steam-compressed wood

As the standard deviations of percentage swelling were less than 0.4%, they are not indicated in Fig. 4 for clarity. The swelling of SC90 was significantly greater than that of the uncompressed wood. The large swelling of SC90 was not due to the irreversible shape recovery, as it had already been boiled in water prior to the swelling-shrinkage test. In addition, the dimensions of SC90 returned to their initial values after the moistening and drying. This confirms that the anomalously large dimensional change in SC90 exhibited in Fig. 4 is a reversible phenomenon. Reversible changes were observed in all the tested SC wood samples. Figure 5 presents the tangential swelling and shrinkage of the uncompressed and SC wood samples as a function of the EMC. As the standard deviations of percentage swelling were less than 0.3%, they are not indicated in Fig. 5 for clarity. The tangential swelling of the SC wood was also reversible. However, in contrast to the radial swelling, it was almost the same as that of the uncompressed wood. In Figs. 6 and 7, the maximum swelling in the R (ΔR_{max}) and T (ΔT_{max}) directions of all the SC samples are compared with those of the uncompressed hardwood samples, respectively. As the standard deviations of the maximum swelling were less than 0.5%, they are not indicated in Figs. 6 and 7 for clarity. The radial swelling of the SC wood was significantly greater than that of the hardwood at the same density, whereas its tangential swelling was almost the same or smaller than that of the hardwood.

These results suggest that the SC wood significantly and reversibly swells and shrinks in its R direction. The dimensional instability of SC wood can be explained by the swimming ring-like expansion and shrinkage of the earlywood

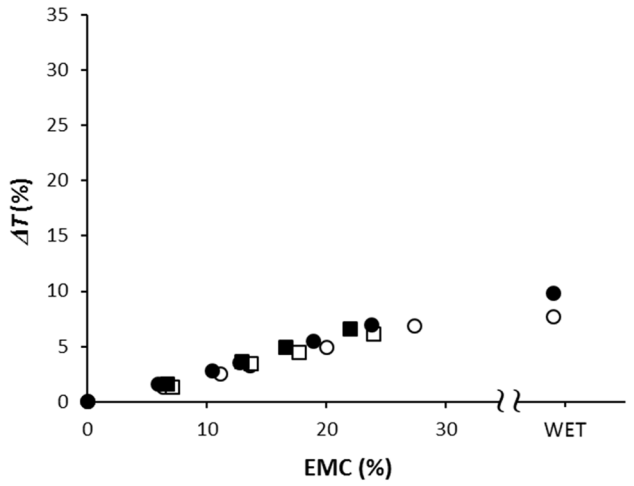

Fig. 5 Swelling in T direction (ΔT) of cedar wood samples as a function of equilibrium moisture content (EMC). Open plots, uncompressed; filled plots, steam-compressed for 90 min (SC90); circles, swelling (moistening) process; squares, shrinking (drying) process, standard deviation was less than 0.3%

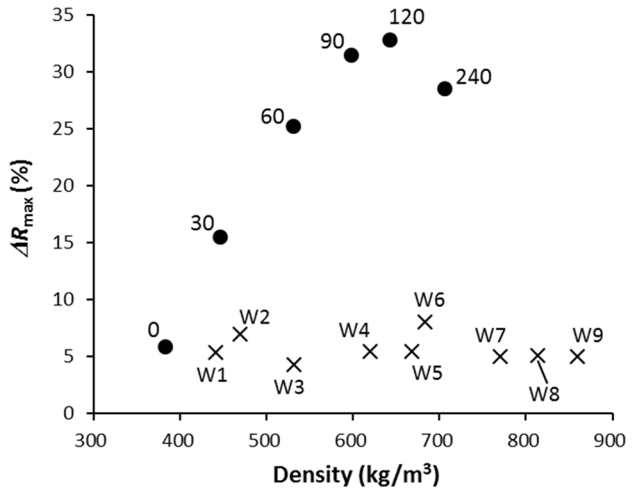

Fig. 6 Maximum swelling in R direction (ΔR_{max}) plotted against wood density. Crosses, uncompressed hardwood (W1–W9); filled circles, steam-compressed (SC) cedar wood. Values beside plots (0–240) indicate steaming duration (unit: min). Standard deviation was less than 0.4% for the uncompressed hardwood or 0.3% for the steam-compressed wood

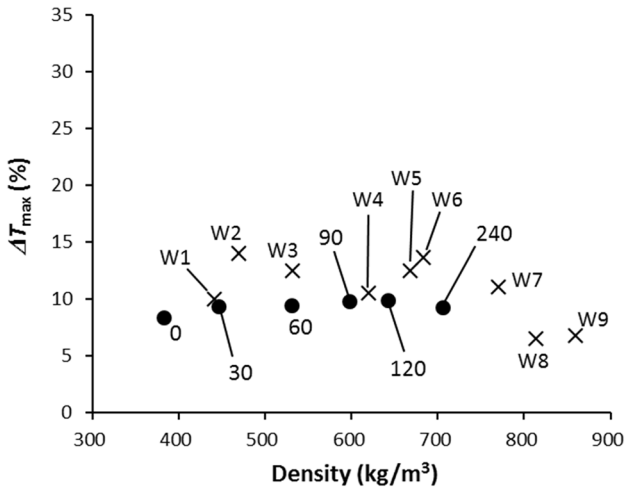

Fig. 7 Maximum swelling in T direction (ΔT_{max}) plotted against wood density. Crosses, uncompressed hardwood (W1–W9); filled circles, steam-compressed (SC) cedar wood. Values beside plots (0–240) indicate steaming duration (unit: min). Standard deviation was less than 0.5% for the uncompressed hardwood or 0.4% for the steam-compressed wood

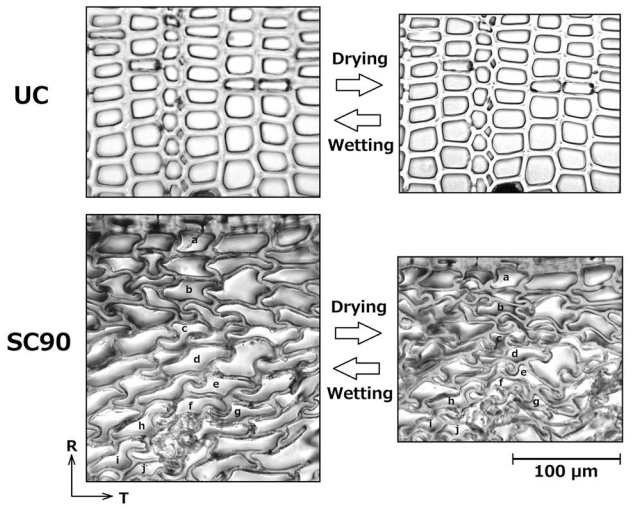

Fig. 8 Cross-sections of earlywood cells of uncompressed (U) and steam-compressed cedar wood (SC90) under wet and completely dry conditions. Alphabets (a–j) in the SC90 indicate the same cells

cells (Obataya and Chen 2018). Figure 8 shows the cross-sections of the earlywood cells in the uncompressed and SC90 samples under the wet and completely dry conditions. It should be emphasized that their dimensional changes were reversible during three cycles of alternate wetting and drying. The cell wall of the uncompressed wood was thickened by the wetting and thinned by the drying, while the cell lumen remained almost unchanged throughout the wetting and drying cycles. In this case, the macroscopic swelling of the wood simply depends on the wood density and moisture content. On the other hand, after the cell wall buckled and was folded by the compression, it was weakened by micro-failures at the folded corner; thus allowing for swimming ring-like inflation by wetting (pumping air into the tube) and a collapse by drying (removal of air from the tube). The cellular deformation may be partially restricted by prolonged steaming (120–240 min) as predicted in Fig. 6. However, prolonged steaming significantly degrades the mechanical performance of wood by the depolymerization and loss of

wood constituents. To prevent the swimming ring-like cellular deformation, the shape of cells must be physically fixed by resin impregnation and intercellular adhesion, similar to that in the fabrication of Compreg (Stamm and Seborg 1944).

3.2 Humidity response of bilayer beam using SC wood

Although the dimensional instability of SC wood is a critical issue in ordinary applications, it is an advantage for humidity-sensitive actuators. Rüggeberg and Burgert (2015) proposed that the combination of different swelling rates in the L and T directions allows for a wooden bilayer beam that deforms in response to changes in the RH. As presented in Fig. 1, the bilayer consisted of a resistant layer and active layer. The length of the resistant layer (L direction of wood) remains almost unchanged, whereas the active layer (T or R direction of the wood) swells and shrinks with changes in the environmental RH. Consequently, the bilayer beam deformed in response to the changes in the RH. According to the results of their theoretical analysis, the swelling rate of the active layer is an important factor that determines the capacity of deflection. Hence, Rüggeberg and Burgert (2015) used beech wood for the active layer, as its tangential swelling is relatively large in common wood species.

As presented in Figs. 6 and 7, the radial swelling of SC90 (32–33%) was higher than the tangential swelling of beech wood (W3, 13%) by a factor of 2.5. This suggests the potential of SC wood as an actuation material that allows for a greater deflection of the bilayer beam. Figure 9 presents the flexural deformation of two bilayer beams, in which SC90 and beech wood were used for the active layers. Greater flexural deformation was achieved by using SC90 instead of beech wood. Figure 10 presents the changes in the environmental temperature, RH, and curvature of the bilayer beams during 3 days of exposure to outdoor conditions. The deformation of the SC90 bilayer was significantly greater than that of the conventional beech wooden bilayer. The results suggest that the SC wood is a useful material for the active layer of a wooden bilayer.

As described in a previous report (Hirano et al. 2016), compressed wood and compressed wood-based composite beams exhibit excellent ductility and elasticity in bending. Therefore, SC wood attracts significant attention due to its increased actuation, ductility, and elasticity. On the other hand, it should be noted that there was a significant decrease in the

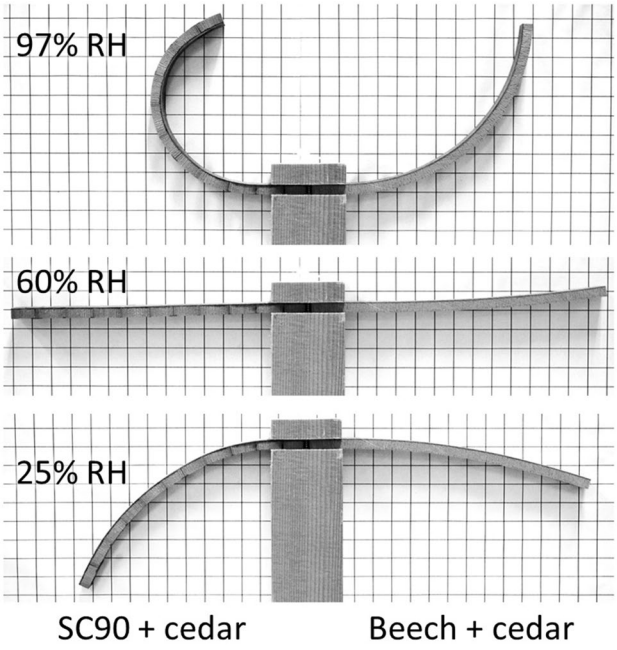

Fig. 9 Flexural deformation of wooden bilayers by moistening at 97% RH and subsequent drying at 25% RH

Young's modulus of cedar wood in the R direction (from 545 to 62 MPa) by radial compression (Chen et al. 2018). It increased to 300 MPa due to steaming, but it was still lower than that of beech wood used in conventional wooden bilayers, which was 500–800 MPa (Rüggeberg and Burgert 2015). Thus, an SC wooden bilayer is not suitable for heavy loads, but recommended for lightweight applications such as humidity-sensitive ventilation flap.

4 Conclusion

Cedar wood was compressed in its R direction, and its compressed shape in dry condition was memorized by steaming at 160 °C. Even after the shape recovery in boiling water, the SC wood exhibited significant and reversible swelling in the R direction due to reversible inflation and the collapse of the earlywood cells. The dimensional instability of SC wood should be considered in ordinary applications. On the other hand, the dimensionally instable SC wood is suitable as a humidity-sensitive wooden actuator. When SC wood was used as an active layer, the wooden bilayer exhibited a larger deflection in response to the environmental humidity than the conventional wooden bilayer.

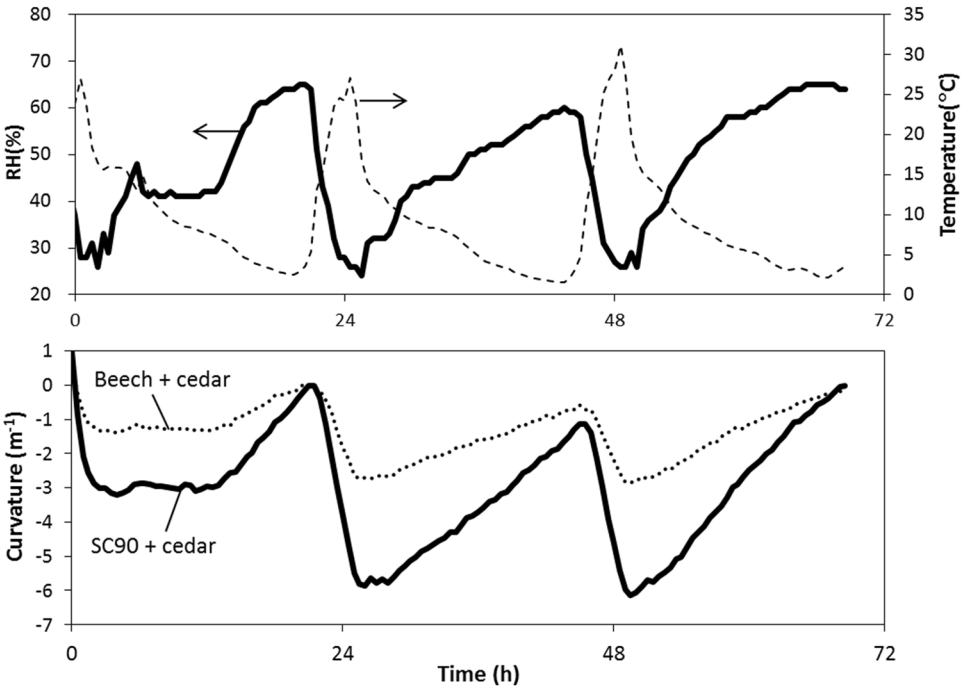

Fig. 10 Changes in temperature, RH, and curvature of wooden bilayers under ambient conditions

Compliance with ethical standards

Conflict of interest On behalf of all authors, the corresponding author states that there is no conflict of interest.

References

Chen S, Obataya E, Matsuo-Ueda M (2018) Shape fixation of compressed wood by steaming: a mechanism of shape fixation by rearrangement of crystalline cellulose. Wood Sci Technol 52(5):1229–1241

Dwianto W, Norimoto M, Morooka T, Tanaka F, Inoue M, Liu Y (1998) Radial compression of Sugi wood (*Cryptomeria japonica* D. Don). Holz Roh Werkst 56:403–411

Fang CH, Mariotti N, Cloutier A, Koubaa A, Blanchet P (2012) Densification of wood veneers by compression combined with heat and steam. Eur J Wood Prod 70:155–163

Guo J, Songa K, Salmén L, Yin Y (2015) Changes of wood cell walls in response to hygro-mechanical steam treatment. Carbohydr Polym 115:207–214

Guo J, Rennhofer H, Yin Y, Lichtenegger HC (2016) The influence of thermo-hygro-mechanical treatment on the micro- and nanoscale architecture of wood cell walls using small- and wide-angle X-ray scattering. Cellulose 23:2325–2340

Guo J, Yin J, Zhang Y, Salmén L, Yin Y (2017) Effects of thermo-hygro-mechanical (THM) treatment on the viscoelasticity of in situ lignin. Holzforschung 71(6):455–460

Hirano A, Obataya E, Adachi K (2016) Potential of moderately compressed wood as an elastic component of wooden composites. Eur J Wood Prod 74:685–691

Inagaki T, Siesler HW, Mitsui K, Tsuchikawa S (2010) Difference of the crystal structure of cellulose in wood after hydrothermal and aging degradation: a NIR spectroscopy and XRD Study. Biomacromolecules 11:2300–2305

Inoue M, Norimoto M, Otsuka Y, Yamada T (1990) Surface compression of coniferous lumber I. A new technique to compress the surface layer. Mokuzai Gakkaishi 36:969–975

Inoue M, Norimoto M, Tanahashi M, Rowell RM (1993) Steam or heat fixation of compressed wood. Wood Fiber Sci 25:224–235

Inoue M, Sekino N, Morooka T, Rowell RM, Norimoto M (2008) Fixation of compressive deformation in wood by pre-steaming. J Trop For Sci 20(4):273–281

Ito Y, Tanahashi M, Shigematsu M, Shinoda Y, Otha C (1998a) Compressive-molding of wood by 1-pressure steam-treatment: part 1. Development of compressively molded squares from thinnings. Holzforschung 52:211–216

Ito Y, Tanahashi M, Shigemitsu M, Shinoda Y (1998b) Compressive-molding of wood by high-pressure steam treatment: part 2. Mechanism of permanent fixation. Holzforschung 52:217–221

Kuribayashi T, Ogawa Y, Rochas C, Matsumoto Y, Heux L, Nishiyama Y (2016) Hydrothermal transformation of wood cellulose crystals into pseudo-orthorhombic structure by cocrystallization. ACS Macro Lett 5:730–734

Kutnar A, Kamke F, Sernek M (2009) Density profile and morphology of viscoelastic thermal compressed wood. Wood Sci Technol 43:57–68

Navi P, Girardet F (2000) Effects of thermos-hydro-mechanical treatment on the structure and properties of wood. Holzforschung 54:287–293

Obataya E, Chen S (2018) Shape recovery and anomalous swelling of steam-compressed wood by swimming ring-like expansion of cell lumina. Wood Sci Technol 52(4):1009–1023

Obataya E, Higashihara T, Tomita B (2002) Hygroscopicity of heat-treated wood III. Effect of steaming on the hygroscopicity of wood. Mokuzai Gakkaishi 48:348–355

Rüggeberg M, Burgert I (2015) Bio-inspired wooden actuators for large scale applications. PLoS One. https://doi.org/10.1371/journal.pone.0120718

Sandberg D, Haller P, Navi P (2013) Thermo-hydro and thermo-hydro-mechanical wood processing: an opportunity for future environmentally friendly wood products. Wood Mater Sci Eng 8:64–88

Seborg RM, Stamm AJ (1941) The compression of wood. Forest Products Laboratory, Forest Service US Department of Agriculture, Madison

Stamm AJ, Seborg RM (1944) Forest Products Laboratory resin-treated, laminated, compressed wood (compreg). For Prod Lab Rep, No, p 1381

Wikberg H, Maunu SL (2004) Characterisation of thermally modified hard-and softwoods by ^{13}C CPMAS NMR. Carbohydr Polym 58:461–466

Yin Y, Berglund L, Salmén L (2011) Effect of steam treatment on the properties of wood cell walls. Biomacromolecules 12:194–202

Yin J, Yuan T, Lu Y, Song K, Li H, Zhao G, Yin Y (2017) Effect of compression combined with steam treatment on the porosity, chemical composition and cellulose crystalline structure of wood cell walls. Carbohydr Polym 155:163–172

Publisher's Note Springer Nature remains neutral with regard to jurisdictional claims in published maps and institutional affiliations.